EUROPEAN FUSION DEVELOPMENT AGREEMENT
JET

EFDA–JET–PR(01)126

F. Zonca, S. Briguglio, L. Chen, S. Dettrick, G. Fogaccia, D. Testa, and G. Vlad

Energetic Particle Mode Stability in Tokamaks with Hollow q-profiles

Energetic Particle Mode Stability in Tokamaks with Hollow q-profiles

F. Zonca, S. Briguglio, L. Chen[1], S. Dettrick[1], G. Fogaccia,
D. Testa[2], and G. Vlad

Associazione EURATOM-ENEA sulla Fusione, C.P. 65-00044 Frascati, Rome, ITALY.
[1]Department of Physics and Astronomy, University of California, Irvine, CA 92697-4575, U.S.A.
[2]Plasma Science and Fusion Center, Massachusetts Institute of Technology, Boston, USA.

Preprint of Paper to be submitted for publication in
Physics of Plasma

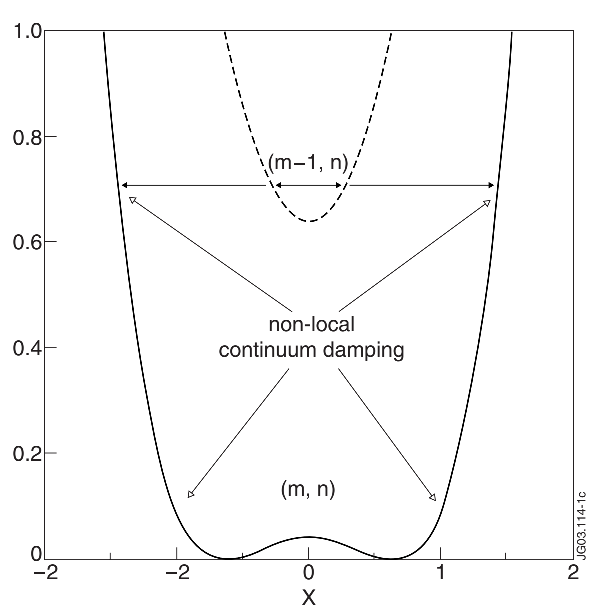

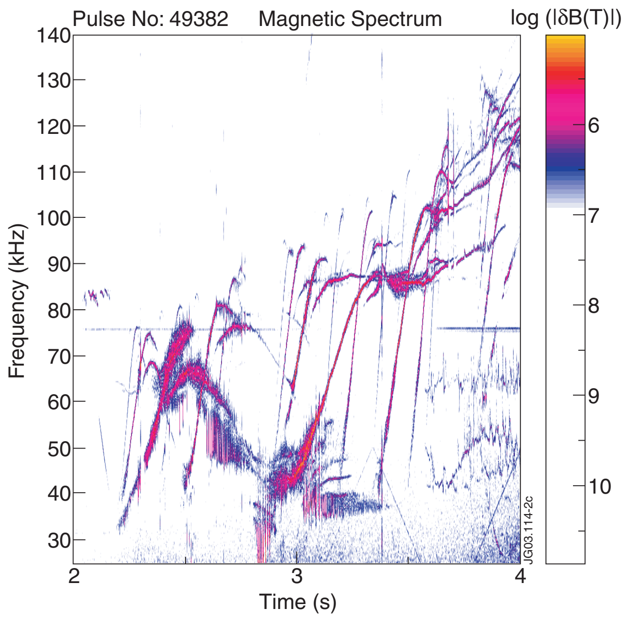

Figure 1: Radial structure of the Shear Alfvén continuous spectrum for the (m, n) and (m − 1, n) modes in the case $r_0/R_0 \langle\langle\ \Omega_{A,m} + \Omega_{A,m-1} \le 1$. The value of $q^2R^2_0\, k_{||}{}^2_{m,\, n}$ is shown vs. $x \equiv \sqrt{nq_0{}^{||}}(r - r_0)$. The frequencies of the (m, n) and (m 1, n) modes are also shown as they are expected from Eq. (3).

Figure 2: Magnetic spectrum in the pre-heating phase of a JET RS plasma with non monotonic q-prole [5]. See also Ref. [6].

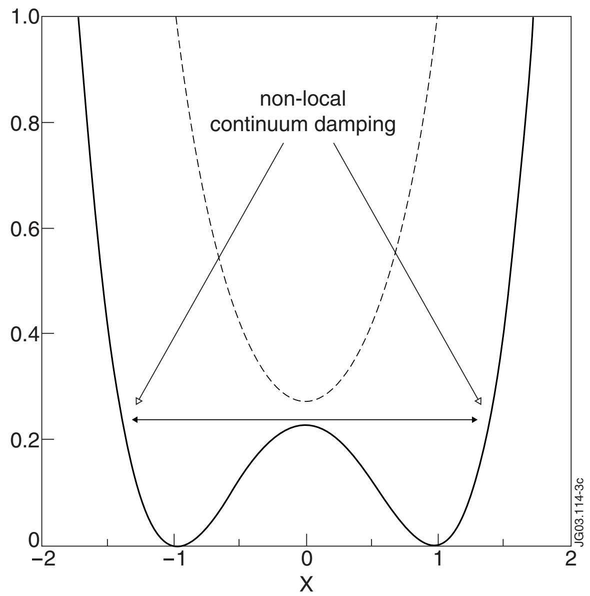

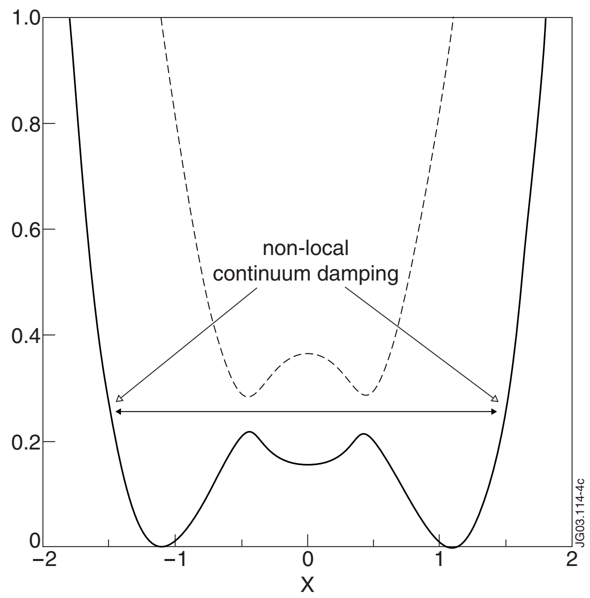

Figure 3: Radial structure of the Shear Alfvén continuous spectrum for the (m, n) and (m − 1, n) modes in the case $\Omega_{A,m} + \Omega_{A,m-1} \approx r_0/R_0$. The value of $q^2R^2_0\, k_{||}{}^2_{m,\, n}$ is shown vs. $x \equiv \sqrt{nq_0{}^{||}}(r - r_0)$. The frequencies of the even parity toroidal mode is also shown as they are expected from Eq. (9).

Figure 4: Radial structure of the Shear Alfvén continuous spectrum for the (m, n) and (m − 1, n) modes in the case $\Omega_{A,m} + \Omega_{A,m-1} \langle\langle\ -r_0/R_0$. The value of $q^2R^2_0\, k_{||}{}^2_{m,\, n}$ is shown vs. $x \equiv \sqrt{nq_0{}^{||}}(r - r_0)$. The frequencies of the even parity double EPM (toroidal mode) is also shown where it could be expected.

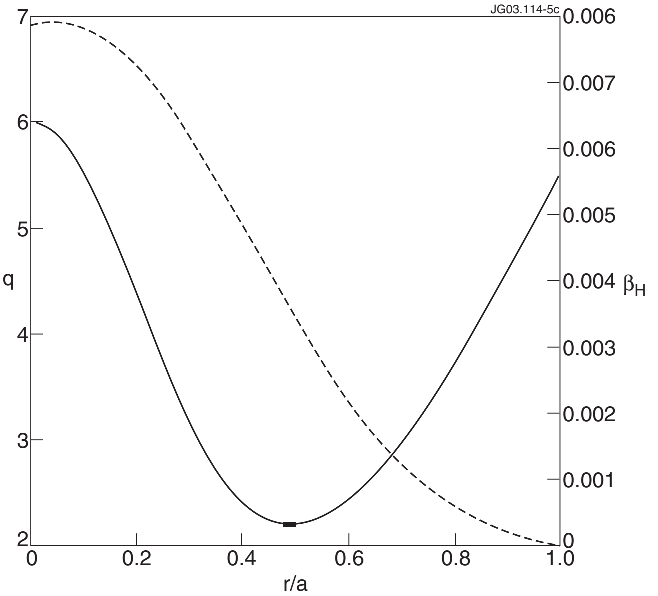

Figure 5: Radial prole for q (solid line) and β_H (broken line).

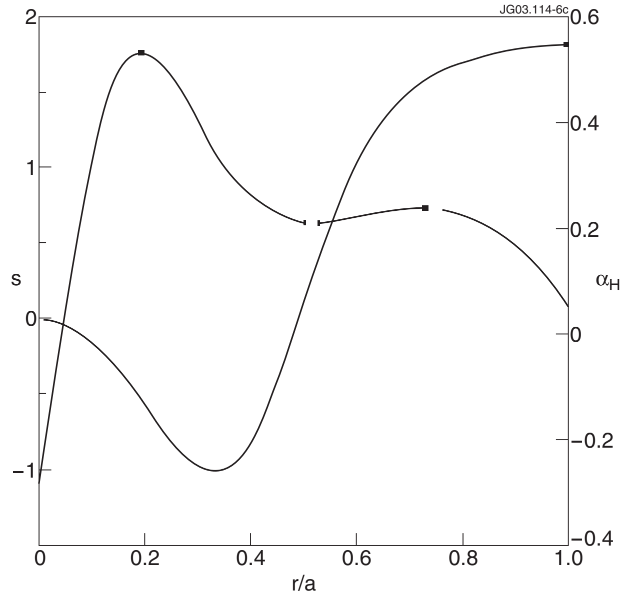

Figure 6: Radial prole for $s = rq'/q$ (solid line) and α_H (broken line).

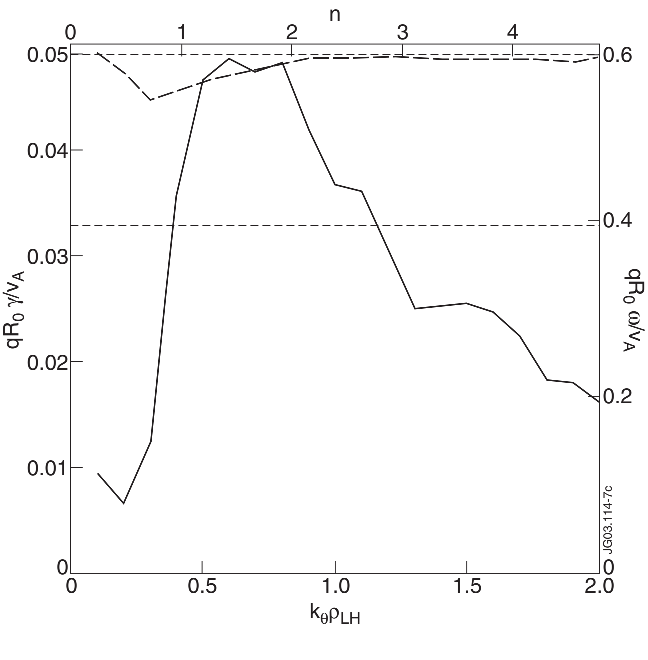

Figure 7: Local values of growth rate (solid line) and real frequency (broken line) of an EPM at r=a = 0:2. The two horizontal lines indicate the toroidal gap in the Alfvén continuum. [5]

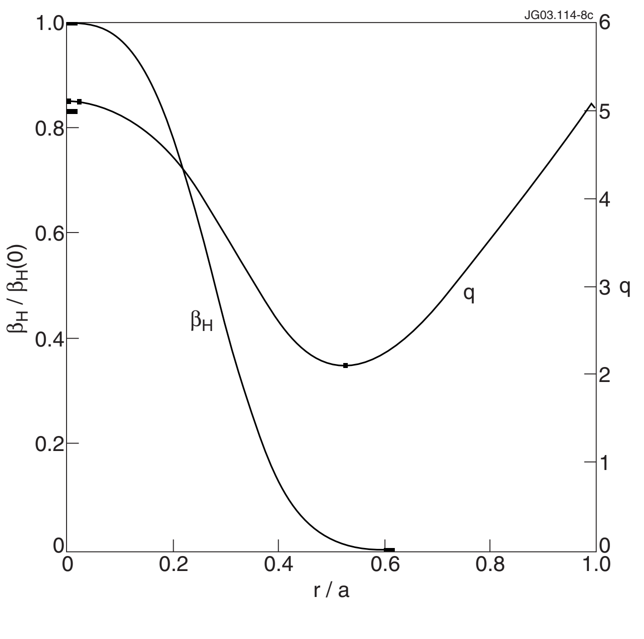

Figure 8: Radial proles of q and β_H that are used in the non-linear simulations with the HMGC code [11, 12].

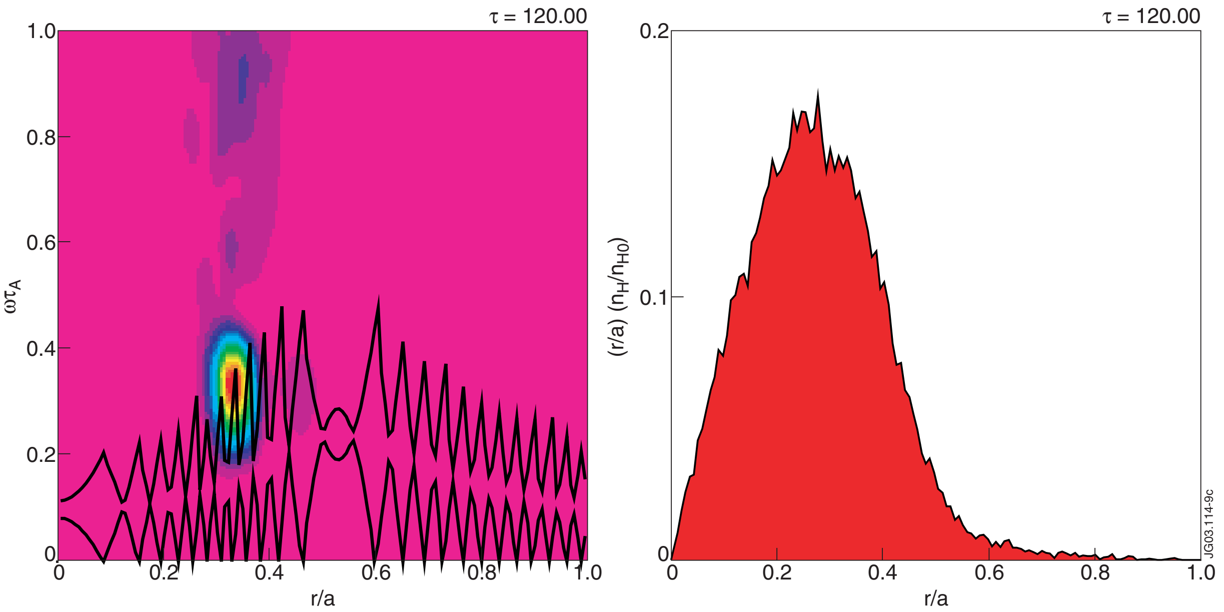

Figure 9: Contour plot (left) of the EPM scalar potential fluctuation intensity in the (r/a, $\omega\tau_A$) plane at $\tau = t/\tau_A = 120$, in the linear destabilization phase. Here, H0 = 0:008 and $\tau_A = R_0/v_A$ is the Alfvén time. The shear Alfvén continuous spectrum is also shown for reference in the background. The initial fast ion radial distribution (right), $(r/a)(n_H/n_{H0})$, is also shown as a function of r/a.

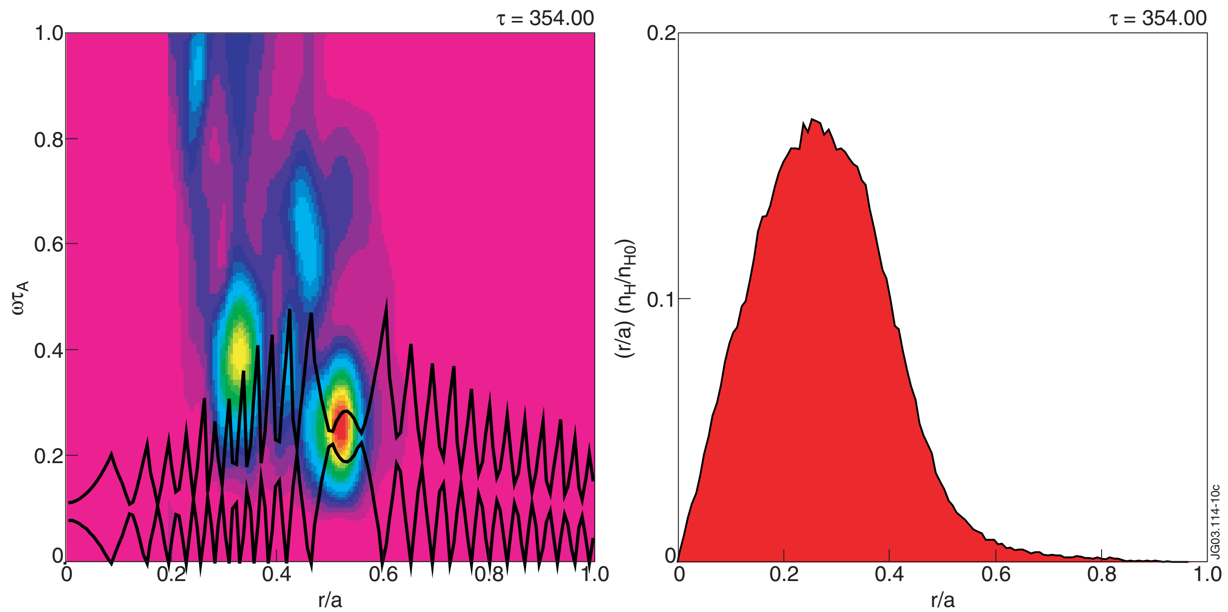

Figure 10: Same as Fig. 9, but at $t = 354\tau_A$, in the fully non-linear saturated phase. The fast ion radial distribution (right), $(r/a)(n_H/n_{H0})$, does not indicate signicant modications from that of the initial state.

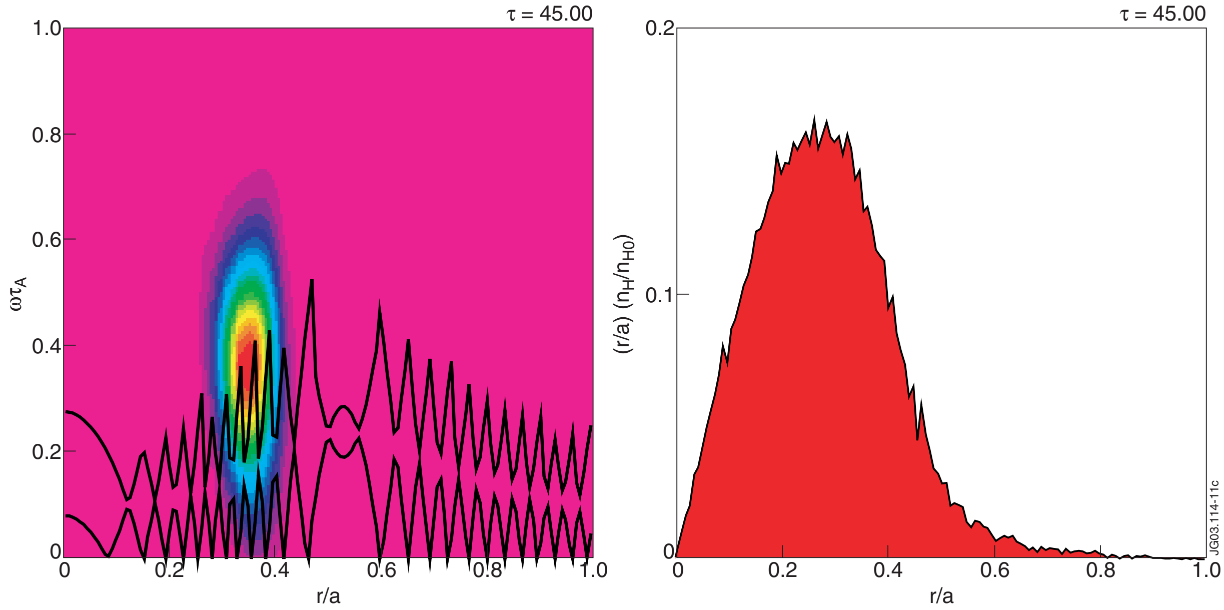

Figure 11: Same as Fig. 9, but with a stronger drive. Here, β_{Ho} = 0:022 and t = 45τ_A, in the linear destabilization phase.

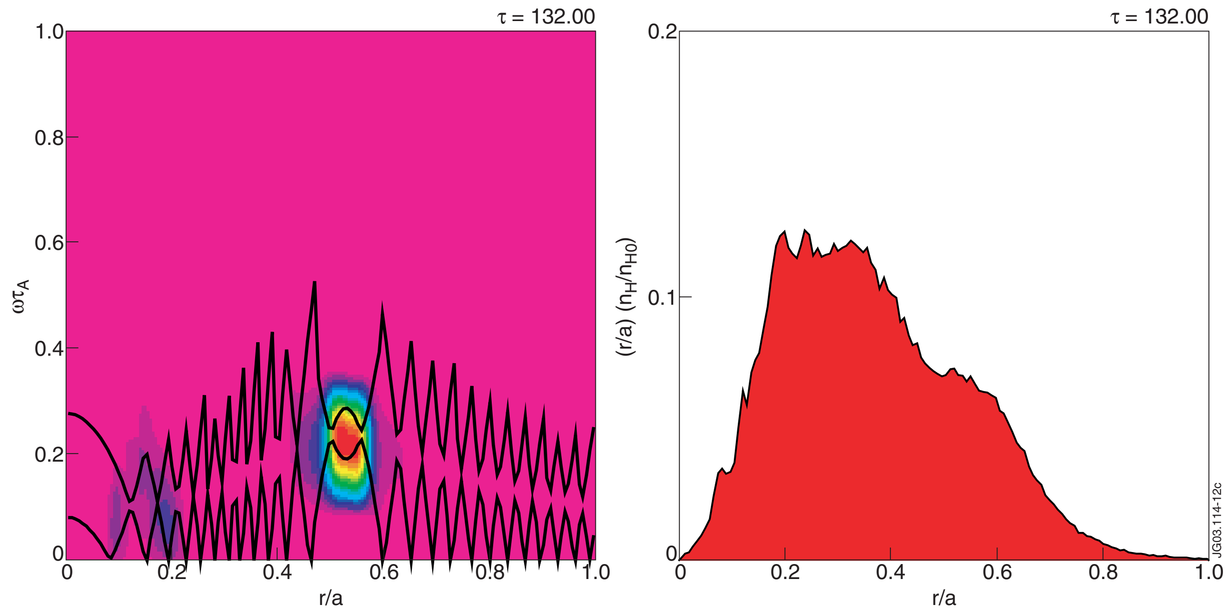

Figure 12: Same as Fig. 11, but at t = 132τ_A, in the fully non-linear saturated phase. The fast ion radial distribution (right), (r/a)(n_H/n_{H0}), shows strong modications when compared with that of the initial state, conrming signicant and rapid radial particle transport.